Hindawi
Journal of Nanomaterials
Volume 2021, Article ID 8617290, 10 pages
https://doi.org/10.1155/2021/8617290

Research Article

Synthesis of Zinc Oxide Nanoparticles by Hydrothermal Methods and Spectroscopic Investigation of Ultraviolet Radiation Protective Properties

Bekele Bulcha,[1] Jule Leta Tesfaye,[2] Degefa Anatol,[3] R. Shanmugam,[4] L. Priyanka Dwarampudi,[5] N. Nagaprasad,[6] V. L. Nirmal Bhargavi,[7] and Ramaswamy Krishnaraj[2,8]

[1]*Department of Physics, College of Natural and Computational Science, Dambi Dollo University, Ethiopia*
[2]*Centre for Excellence-Indigenous Knowledge, Innovative Technology Transfer and Entrepreneurship, Dambi Dollo University, Ethiopia*
[3]*Department of Mathematics, College of Natural and Computational Science, Dambi Dollo University, Ethiopia*
[4]*TIFAC CORE HD, Department of Pharmacognosy, JSS Academy of Higher Education and Research, JSS College of Pharmacy, Ooty, Tamilnadu, India*
[5]*Department of Pharmacognosy, JSS Academy of Higher Education and Research, JSS College of Pharmacy, Ooty, Tamilnadu, India*
[6]*Department of Mechanical Engineering, ULTRA College of Engineering and Technology, Madurai, 625 107 Tamil Nadu, India*
[7]*Department of Chemistry, Sri Venkateswara College of Engineering and Technology, 517004, Chittoor, Andhra Pradesh, India*
[8]*Department of Mechanical Engineering, Dambi Dollo University, Ethiopia*

Correspondence should be addressed to Ramaswamy Krishnaraj; prof.dr.krishnaraj@dadu.edu.et

Received 20 June 2021; Revised 9 August 2021; Accepted 1 September 2021; Published 23 September 2021

Academic Editor: Lakshmipathy R

Ultraviolet radiation causes damages to the human body, such as skin ageing, skin cancer, and allergies throughout the world. Applying zinc oxide nanoparticles (ZnO NPs) in sunscreen products (like cloths or textiles) to protect human skin by absorbing the ultraviolet radiations that emerged from the sun. The main aim of this study is to investigate both absorbance and transmittance characteristics of the untreated and treated cotton textiles. For ZnO NPs using hydrothermal methods, they were made from $Zn(NO_3)_2{\cdot}6H_2O$ and NaOH at a constant annealing temperature of 300°C. Fourier transform infrared (FT-IR), X-ray diffraction (XRD), scanning electron microscopy (SEM), and UV-vis spectroscopy were used to analyze the produced ZnO NPs. From the FT-IR result, ZnO NPs were observed in the region of 400-600 cm^{-1}. Wurtzite hexagonal structure of ZnO NPs with the average crystal size 32 ± 49 nm was observed from XRD results. Flowers in the shape of synthesized ZnO NPs were observed from SEM images. The UV-vis penetration peaks were identified at 264 nm and 376 nm, with energy band gaps of 4.68 and 3.536 eV, respectively. When compared to bulk ZnO, the energy band gap of ZnO NPs was blue-shifted due to the impact of quantum confinement. The peaks in UV-vis absorption were caused by an electronic transition from the valiancy to the conduction bands. The high energy band shows high absorbance of the synthesis sample in the case of 264 nm. The ZnO NPs were manufactured and applied to 100% of raw cotton to impart sunscreen action to both untreated and treated cotton fabrics. The performance of treatment has been evaluated utilizing UV-vis spectroscopy through quantifying ultraviolet protective factors (UPF) and percentage of transmitted (%T) radiations. The treated cotton textiles have 61.50% UPF while 2.65% ultraviolet radiations were transmitted. In other words, untreated cotton textiles have 1.63% UPF while 74.56% ultraviolet radiation was transmitted. Therefore, the treated cotton textiles have excellent protection categories when compared to untreated cotton textiles.

1. Introduction

Nanotechnology is a new field of study that deals with the discovery and use of nanoparticles containing structural differences among the nanomaterials with their bulk counterparts. It also refers to the art and science of creating and using nanoparticles having fundamental properties and functions [1]. Nanoparticles are microscopic particles with a diameter of 1 to 100 nanometers that are used in current textile technology. Nanoparticles also have a wide range of applications in life science [1, 2], biomedical [3, 4], healthcare [4], and security [5] as well as the energy generation [6], farming [7], sustainable energy [6, 7], energy storage [6, 8], infrastructure [9], and building and constructions [10]. Because of their capacity to transfer charges and give fast responses, as well as their ease of use and inexpensive cost, ZnO NPs are a popular choice among nanoparticles for a range of applications. According to the literature [2–4, 7, 11], ZnO NPs can be used in textiles as UV blocking properties, antifungal, antibacterial activities, solar screening, cosmetics, food packaging, biomedical, self-cleaning, water, and air cleaning, sterilizing surroundings, and photocatalyst due because of its one-of-a-kind physical and chemical characteristics such as high electrochemical coupling coefficient, more chemical stability, a diverse range of absorbing radiation, huge excitonic binding energy (60 meV), large energy band gap (3.37 eV), and high mechanical and thermal stability. ZnO NPs have a number of great qualities, including ease of synthesis, controllable shape and size, nontoxicity, the existence of extrinsic and intrinsic at the emission centre, and the ability to emit a variety of hues (violet, blue, green, yellow, and red) [12–14].

UV radiation protection is one of the most critical challenges in the textiles industry because of ozone depletion and the greenhouse effect. Ultraviolet radiation penetrates from the sun to the earth in the form of energy having fifty percent visible lights, forty-five percent infrared, and five percent ultraviolet radiations [15]. UV radiation can be classified into three wavelength regions based on its wavelength: UVA (400 nm-320 nm), UV-B (320 nm-280 nm), and UV-C (280 nm–200 nm) [3, 5, 7]. At this time, the ozone layer has completely absorbed UV-C. From all UV radiation, the most damaging types of radiation are UV-A and UV-B. It has high energy and a short wavelength [4–6, 15]. In order to reduce such effects, ZnO NPs must be synthesized for textiles industries. Cubic rock salt, cubic zinc blende, and hexagonal are the three most common structures of ZnO NPs. Under normal environmental circumstances, hexagonal structures are thermodynamically stable [7]. Nanowire, nanoflower, nanocombs, nanobelts, nanocages, nanosprings, nanoring, needle-like, nanoflake, spherical, nanohelix, sheet, bullet-like, hexagonal plate, polyhedral, nanotube, nanorod, pyramid shape, doughnut-like, malty sphere, nanobows, nanoleafs, star, spike, and multipods, smashed stone-like, cylinder-like, and ellipsoid are morphological forms of ZnO NPs derived from SEM [5–8, 12–16]. UV radiation absorbance by semiconductive, whether significantly refractive or dispersing radiations, is closely related to the UV blocking characteristics of ZnO NPs. The chemical composition of ZnO NPs has a direct impact on their protective actions [11, 16]. Furthermore, particle shapes, sizes, crystals, and crystalline forms all have a role [9–13]. When textiles are subjected to UV radiation, they experience direct transmittance, absorption, and scattering [13]. Skin damage is caused by UV radiation that is emitted, as well as reflection and fibre dye [10–13]. UV radiation absorption is measured inside ultraviolet protective factors (UPF). The UPF value of treated fabrics evaluates their blocking qualities, and the greater the UPF value, the much more protective they are [10]. For the production of ZnO NPs, a range of preparation techniques have been reported, including chemical precipitation, spray-pyrolysis, hydrothermal, sol-gel, photochemical, and electrospanning methods [13, 14, 16–20]. As reported in several kinds of literature [6], ZnO NPs were prepared for textile application through hydrothermal methods using different solvents (distilled water, ethanol, and methanol) results from 20 to 9 nm sizes with high UPF of UV-A and UV-B. Recently, ZnO NPs were prepared for UV absorber properties of cotton textiles using zinc acetate $(CH_3COO)_2{\cdot}2H_2O$) and NaOH precursor by adding surfactant (cetyl trimethyl ammonium/CTAB) was seen in literature [12]. Yadav et al. [21] prepared ZnO NPs with an average diameter of less than 35 nm for cotton textiles results from an increment of UPF and antimicrobial activities. Another group of researchers leads by Ibrahim et al. [22] also prepared ZnO NPs by sol-gel technique for cotton textiles found 359 nm of particle size which provides durable multifunctional fishing (UV protection and antimicrobial activities).

Several kinds of literature use sol-gel methods to prepare ZnO NPs rather than hydrothermal methods, and there are no clear methods to prepare ZnO NPs using hydrothermal processes. Previously, no literature reports on the comparison of absorbance of untreated and treated cotton textiles and a transmittance of untreated and treated cotton textiles. Furthermore, a comparison of transmittance with an absorbance of treated and untreated cotton textiles was not clearly reported previously. Therefore, this research gives detail information on synthesis methods and UV-protective properties of nanoparticles in terms of absorbance and transmittance. ZnO NPs were prepared using $Zn(NO_3)_2{\cdot}6H_2O$ and NaOH precursors. The produced samples were FT-IR analyzed and utilized to identify contaminants. The XRD results demonstrate that the ex situ produced nanoparticles [17], which have been deposited onto bleached cotton fibers, had an average weight of 33 nm, as reported in various literature. SEM is used to analyze the shape of the nanoparticles, and a UV-vis is accustomed to evaluate the absorption spectrum of untreated and treated cotton textiles [18–46]. As a result, the goal of this study is to synthesize, characterize, contrast, and compare untreated and treated cotton textiles.

2. Experimental Details

Sodium hydroxide (NaOH), zinc nitrate hexahydrate $(Zn(NO_3)_2{\cdot}6H_2O)$, and ethanol were acquired from a local supplier (used without further purification). ZnO NPs were made utilising a hydrothermal method that included the use of $Zn(NO_3)_2{\cdot}6H_2O$ and NaOH precursors, as described

in the literature [18]. For this situation, a 0.6 M aqueous ethanol solution of $Zn(NO_3)_2{\cdot}6H_2O$ were maintained with constant stirring for 45 minutes with a mild magnetic stirrer to thoroughly dissolve the zinc nitrate hexahydrate, and a 1 M aqueous ethanol solution of NaOH was likewise made exactly the same as 45 minutes of agitation. After the zinc nitrate hexahydrate was completely dissolved, 1 M NaOH mixture was prepared by slowly adding drop by drop for 25 minutes without touching the container's wall, while magnetic stirring was kept at high speed. The process was permitted to continue for 1 hour after the aqueous solution of NaOH was added, and the container was sealed at this temperature for 1 hour. Afterward, the sample was transferred to settle for an overnight period before the resultant liquid was carefully separated. The precipitate was removed after 15 minutes of centrifugation. ZnO NPs were precipitated and rinsed four times with the double distilled water and ethanol before being dried in an air environment at roughly 90°C. Zn $(OH)_2$ was totally transformed to ZnO NPs at this time, and the existence of nanoparticles and other functional groups was determined by Fourier transform infrared spectroscopy (FT-IR). The size, shape, optical, and structural properties of the produced ZnO NPs were all measured. An X-ray diffractometer (panalytical) was used to record the X-ray diffraction (XRD) pattern of manufactured ZnO NPs using Cu-K radiation with a wavelength of ($\lambda = 0.1541$ nm) in the scan range of 2theta = 10°–80°. A scanning electron microscope (SEM) with (EDXA, SIRION) for the morphology of the specimen was examined using compositional analysis of generated ZnO NPs. Using a UV-vis spectrophotometer (Hitachi, U-3010), the optical transmission/absorption spectra of ZnO NPs distributed in water were recorded as follows. The solution was dipped in a quartz cuvette and taken into a UV-vis spectrophotometer with around 0.3 g of ZnO NPs dissolved in deionized water. In such a process, the absorbance/transmittance spectra of ZnO NPs were measured. Finally, ZnO NPs were brought into the application as follows. White 100% cotton fabrics were purchased from the local market of Dambi Dollo Town, Oromia Regional State. A piece of cotton textiles with a surface area of 10 cm × 10 cm and a mass for every unit surface of 60 g m^{-2} were prepared and washed five times using deionized water. Then, the fibre was soaked by ZnO NPs solution for 10 min by a gentle magnetic stirrer. The cloth was dried in the oven at 130°C for 15 min to remove the excessive dispersion. UV/absorption and transmission were then used to determine the efficiency of the shielding against UV radiation.

3. Results and Discussion

This current research includes the development of nanoparticles by hydrothermal approaches that aid in the management of surface energy. FT-IR, XRD, SEM, and UV-visible spectroscopy were used to characterize the functionalized nanoparticles. The nano and other potential functional groups of produced ZnO NPs were investigated using Fourier transform infrared (FT-IR). FT-IR transmission spectra of ZnO NPs in the 400–4000 cm^{-1} range were measured, as shown in Figure 1 below. The stretching vibration of O-H has appeared at 3428 cm^{-1}, and this is maybe due to the oscillation of water molecules [14, 17, 19, 21]. The peak observed at 2924 cm^{-1} was related to –CH2 vibration [21, 23]. The transmission peaks were observed at 1557 cm^{-1} due to C=O symmetric stretching [22]. The transmission peaks observed at 1391 cm^{-1} and 1278 cm^{-1} were bending, and the vibrational mode of CO_2 was related to CO_2 is from the real environment [18]. The peak observed at 1055 cm^{-1} was associated with H-O-H bending vibration was due to the presence of water of crystallization [25]. The band observed at 810 cm^{-1} was also due to the deformation vibration of water molecules [21–23]. The transmission band observed at 466 cm^{-1} was due to Zn-O stretching mode [27].

The XRD diffraction spectra of prepared ZnO NPs were shown in Figure 2 below. ZnO NPs were prepared from zinc nitrate hexahydrate ($Zn(NO_3)_2{\cdot}6H_2O$) and sodium hydroxide (NaOH) through hydrothermal methods. A broad and well-defined spectral peaks show that the synthesized substances incorporate particles in the nanoscale range. Intensity, full-width at half-maxima, size, and position were determined from XRD result analysis. About nine diffraction peaks were observed at 21.77°, 24.43°, 26.26°, 37.55°, 46.62°, 52.88°, 56.40°, 57.97°, and 59.1° with their corresponding crystal plane of (100), (002), (101), (102), (110), (103), (200), (112), and (201), respectively. Broad diffraction and most intense peak peaks without peak shift were observed at (101) peaks. Randomly oriented crystallites were seen from these several peaks.

The average crystallite size (D) of produced ZnO NPs were estimated via the Debye-Scherrer formula (1).

$$D = \frac{0.89\,\lambda}{\beta \cos\theta}, \tag{1}$$

where D is the crystallite size, λ is the X-ray transmittance wavelength ($\lambda = 0.15418$ nm), β is full-width at half-maximum (FWHM) in radians, and θ represents the angle of diffraction [20]. Table 1 displays the average particle size distribution of produced ZnO NPs, which was about 32.49 nm.

The produced material has a size range of 1 nm to 100 nm and is suitable for use in the textile industry [21]. The measured "D" values for ZnO nanopowder or synthesized nanomaterials have crystallized in a hexagonal wurtzite structure, as shown in Table 1, are also in excellent accordance with all those obtained from Joint Committee on Powder Diffraction Guideline (JCPDS) card document data for ZnO nanopowder or synthesized nanomaterials [5, 9].

The lattice spacing (d) were derived from Braggs equation:

$$d = \frac{\lambda}{2 \sin\theta} \tag{2}$$

The lattice parameters c and a were determined from

$$a = \sqrt{\frac{1}{3}}\frac{\lambda}{\sin\theta}, \tag{3}$$

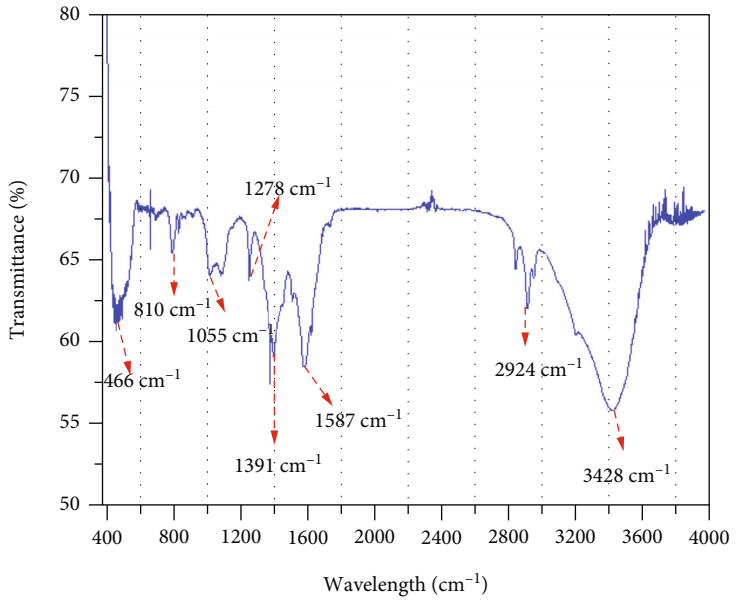

Figure 1: Fourier transform infrared (FT-IR) spectral analysis of prepared ZnO NPs.

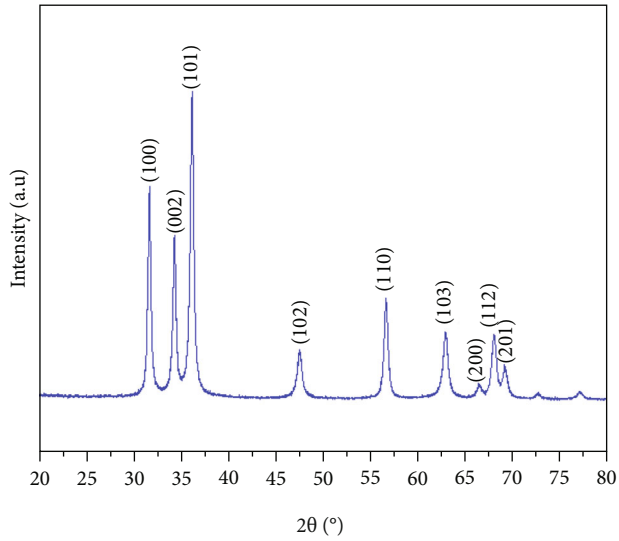

Figure 2: X-ray diffraction (XRD) pattern of prepared ZnO NPs.

Table 1: Diffraction angle (2theta), FWHM (β), and average crystallite size (D) of prepared ZnO NPs.

No.	2theta (degree)	Cos2θ (radian)	β (radian)	β (Cos2θ)	Crystallite size (nm)	Average D (nm)
1	21.77	0.0162	0.269	0.0043	31.90	
2	24.43	0.0159	0.278	0.0044	31.18	
3	26.26	0.0156	0.298	0.0046	29.82	
4	37.55	0.0138	0.365	0.0050	27.44	
5	46.62	0.0119	0.355	0.0042	32.67	32.49
6	52.88	0.0105	0.417	0.0043	31.90	
7	56.40	0.0096	0.377	0.0036	38.11	
8	57.97	0.0096	0.426	0.0040	34.30	
9	59.10	0.0089	0.442	0.0039	35.17	

Table 2: Lattice parameters, lattice spacing, unit cell volume, grain size, and dislocation density of prepared ZnO NPs.

Hkl	Lattice parameter			Lattice spacing	Unit cell volume (nm)	Grain size (δ)	Dislocation density (ε)
	a (nm)	c (nm)	c/a (nm)				
101	0.3617	0.3899	1.0779	0.339	0.0442	0.0668	7.1063

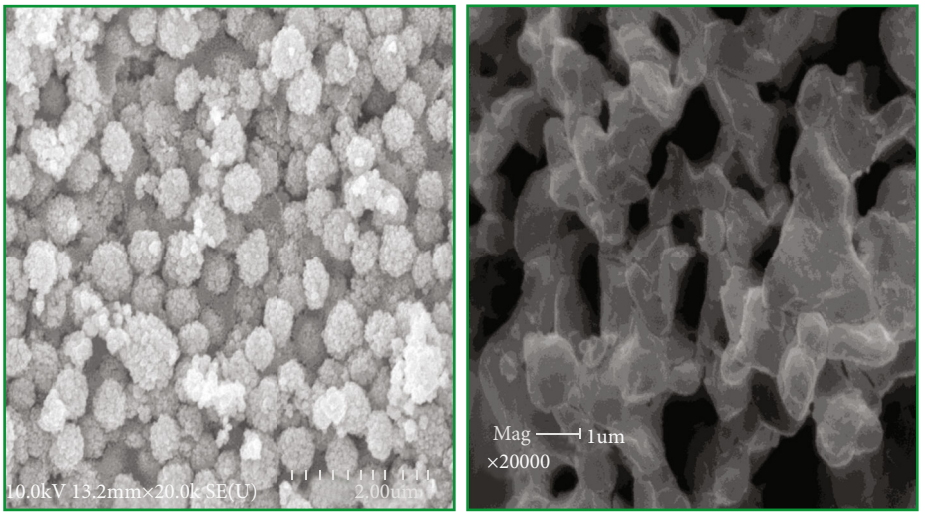

Figure 3: Scanning electron microscopy (SEM) images of synthesized ZnO NPs with different magnifications.

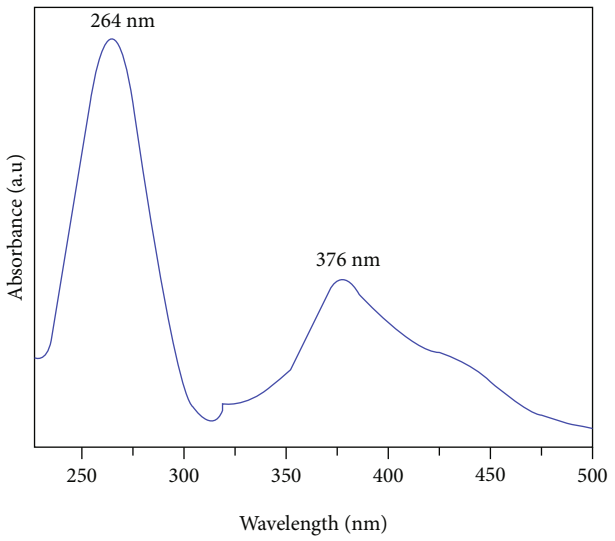

Figure 4: Absorption spectral analysis of synthesized ZnO NPs.

$$c = \frac{\lambda}{\sin\theta}. \quad (4)$$

The unit cell volume (V)

$$V = \frac{\sqrt{3}}{2}a^2c. \quad (5)$$

The grain size (δ) of synthesized particles were evaluated by using the following formula:

$$\varepsilon = \frac{\beta\mathrm{Cos}\theta}{4}. \quad (6)$$

The dislocation density (δ) is used to determine the defects in crystallite were determined from Small man's and Williamson formula.

$$\delta = \frac{15\varepsilon}{ad}. \quad (7)$$

The grain size and dislocation density of the synthesized sample were obtained from peak of XRD and summarized in

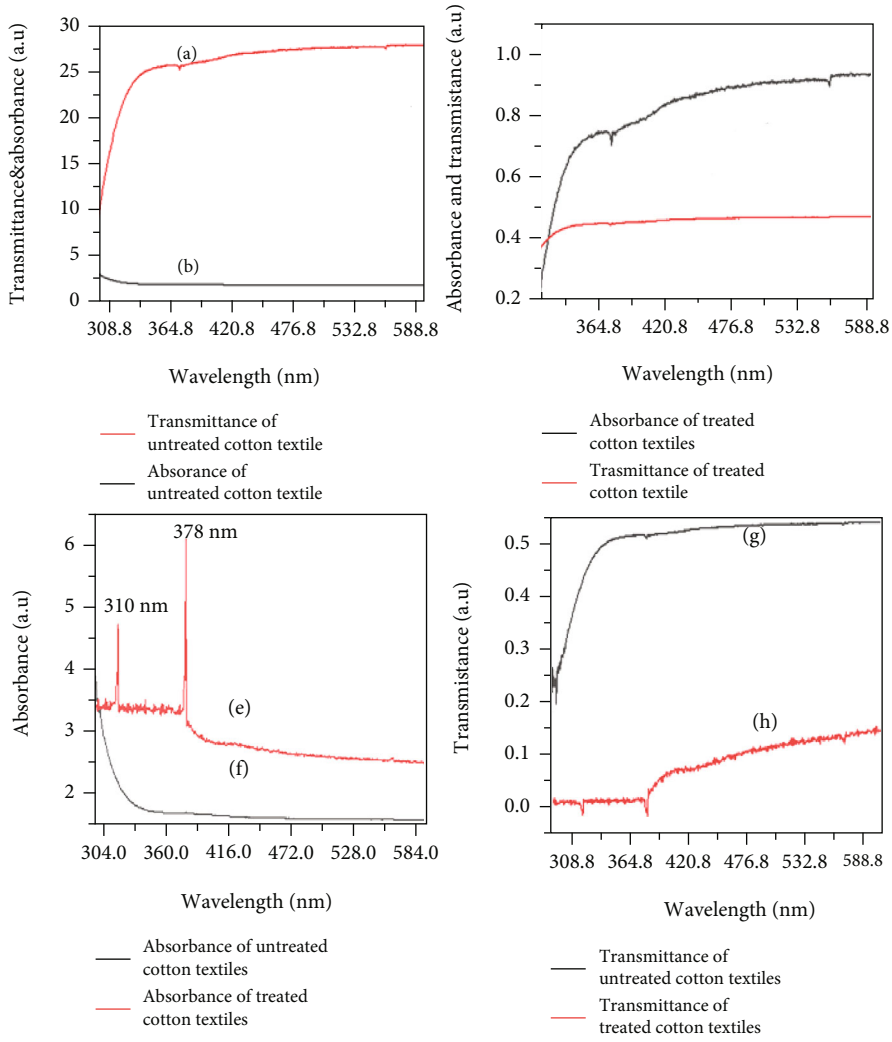

Figure 5: UV-vis spectral analysis: transmittance and absorbance of untreated cotton textiles (a, b) and nanotreated cotton textiles (c, d). The absorbance of treated and untreated textiles (e, f) and transmittance of untreated and treated textiles (g, h).

Table 2 above. As described in JCPDS card number 36-1451, all X-ray diffraction peaks of manufactured ZnO NPs are carefully categorized of wurtzite structure with lattice parameters of $a = b = 0.3249$ nm and $c = 0.5206$ nm. For (101) peaks, the lattice parameters 'a' and 'c,' spacing distance (d), and volume cell of ZnO NPs were computed, and there was a minor variance in the lattice parameter values. The variation could be caused by a minor shift throughout the position of its peaks as a result of a fault [22, 23]. Lattice imperfection of synthesized nanoparticles was observed from dislocation density and strain. Figure 3 represents the SEM image of prepared ZnO NPs at a constant annealing temperature of 300°C. The particle morphology is homogenous and well spread, with a flower-like shape. This shows that ZnO NPs may be successfully produced utilising zinc salt precursors in the nanoscale range.

The UV-vis absorbance spectrum of produced ZnO NPs at a fixed heating rate of 300°C is depicted in Figure 4. These uptake peaks were found at 264 nm and 376 nm. The strong absorption peak was observed at 264 nm. This indicates that a high ability to absorb ultraviolet radiation. Furthermore, synthesized nanoparticles have high absorption abilities in the region of 200-300 nm and 350-450 nm.

The technique of UV-vis absorption spectroscopy is commonly adapted to investigate the optical characteristics of particles that are in nanosize [33]. The ZnO nanoparticles, which are substantially underneath the bandgap frequency of 376 nm, give rise to an excitonic maximum absorption at roughly 264 nm ($E_g = 3.29$ eV). The fact that considerable sharp absorption of ZnO implies that the nanoparticle dispersion is monodispersed [7]. The bandgap energy of the synthesized samples was computed by using the absorption edge relationship equation (8) [24–27].

$$E_g = h\nu_g = \frac{hc}{\lambda_g}, \tag{8}$$

where $h = 4.14 \times 10^{-15}$evs, $C = 2.99 \times 10^{8}$m s^{-1}, and its wavelength.

The E_g values for samples were 4.68 and 3.13 eV, which are in good accordance with the literature. In comparison to

Table 3: UV blocking qualities of the handcrafted cotton fabrics.

Specimens	Transmittance (%)	UPF	Protection categories
Treated	2.65	61.50	Excellent
Untreated	74.56	1.63	Neat

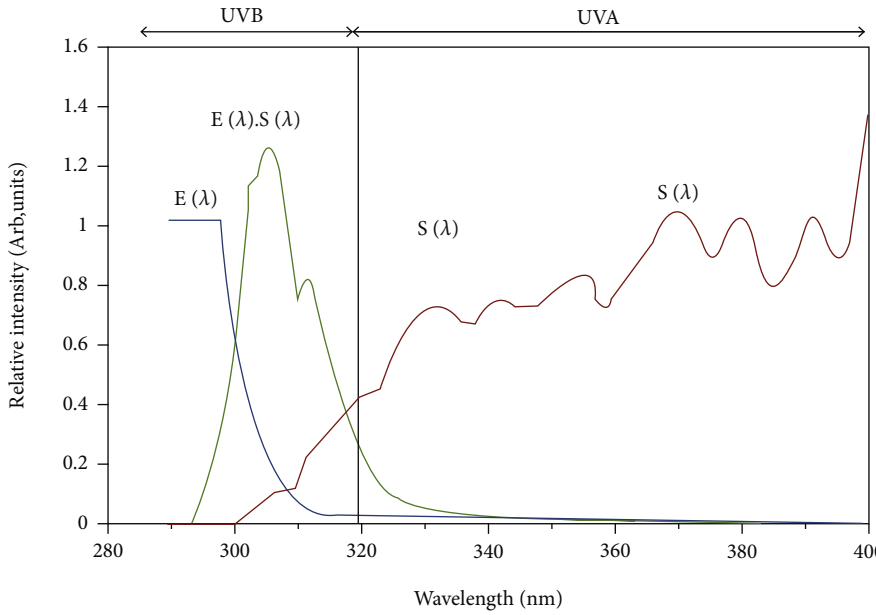

Figure 6: Graph of relative erythermal action spectrum, $E(\lambda)$, standard solar spectral irradiance, $S(\lambda)$, and $E(\lambda) \cdot S(\lambda)$ in the ultraviolet light region.

bulk ZnO, the quantum confinement impact pushed its energy band gap of ZnO nanoparticles to the blue. Peaks have been caused due to electronic transition from the valence band to the conduction band. The use of nanosized ZnO NPs on 100 percent cotton fabrics enhances UV/radiation absorption. ZnO NPs have been applied to the surface of cotton fibres. The ability of ZnO NPs to absorb UV rays was successfully transferred to fabric products. The absorbance and transmittance spectra of untreated and treated cotton fabric in the 200-500 nm range are shown in Figure 5. Highly transmitted ultraviolet radiation was observed from untreated cotton textiles, as shown in Figures 5 and 5(b). As shown in Figures 5(c) and 5(d), more ultraviolet radiation was absorbed rather than transmitted. A small amount of radiation was transmitted through nanocotton textiles that have been treated [47].

The absorption ability of treated and untreated textiles was shown in Figures 5(e) and 5(f). Higher values of ultraviolet absorbance were obtained when cotton textiles were treated with ZnO NPs. The sensitivity of treated cotton fabrics was shown to be higher at 378 nm and 297 nm, which are both in the UV range, while untreated cotton textile (see Figure 5(f)) does not absorb ultraviolet radiation. The transmittance ability of untreated and treated cotton textiles was observed in Figures 5(g) and 5(h), and a low ultraviolet radiation spectrum was transmitted through nanocoated cotton textiles. The wash withstanding ability of nanoparticles is an intriguing feature of their treatment. After 25 washes, the treated fabrics were examined again because there was no discernible difference in their sunscreen activity. This clearly shows that even without the application of a binder, the nanoparticles are strongly attached to the cloth surface. A binder, on the other hand, can be employed when a higher degree of wash fastness is necessary [14, 16, 24–27]. As shown in Table 3, the UV protection parameter (UPF) and percent transmittances (%T) were determined using equations (9) and (10), respectively.

$$\text{UPF} = \int_{\lambda 1}^{\lambda 2} \frac{E(\lambda).S(\lambda)}{E(\lambda).S(\lambda).T(\lambda)} d\lambda, \quad (9)$$

$$\%\text{Transmition} = \sum_{\lambda 1}^{\lambda 2} \frac{T(\lambda)}{\lambda 2 - \lambda 1}. \quad (10)$$

In this case, $E(\lambda)$ is relatively erythermic spectral efficiency, $S(\lambda)$ in $\text{Wm}^{-2}\,\text{nm}^{-1}$ is a specimen of spectrum transmittance produced from UV spectrometric tests, and $E(\lambda)$ and $S(\lambda)$ were acquired at the national database of sea surface temperature administration (NOAA), [18, 29], which is shown in Figure 6 [31–35].

Tests for UV-A and UV-B are generally conducted in the UVA and UVB zones. However, $E(\lambda)$ has very tiny UV-A values and is substantially large in the UV-B field, as seen

in Figure 6. Therefore, the UPF value indicates mostly UVB protection rather than a wide range of protection against UVA-UVB [36–43].

The use of ready ZnO NPs on cotton fabrics improves the absorption and transmission of UV light. This means that UV radiation shields are effectively absorbed by ZnO NP UV radiation upon its cotton textile surface. As ZnO NPs treat cotton has a small percentage of the transmission, untreated materials have a high percentage of the transmission (Table 3).

It was proven by the variety of cotton textiles that, compared to cotton-treating textiles, a considerable % of transmittance in unprocessed textiles having a low ability to block ultraviolet light, i.e., unprocessed cotton textiles absorb ultraviolet radiation. In comparison with untreated cotton textiles, the low spectrum in the transmission of cotton textiles has shown a significant UV blocking capability [16, 22, 30].

4. Conclusion

Sodium hydroxide and zinc nitrate hex-hydrate were used to create ZnO NPs using a hydrothermal technique. Different characterization tools were used to characterize the produced ZnO NPs. These instruments are Fourier transform infrared (FT-IR), X-ray diffraction (XRD), UV-vis spectroscopy, and scanning electron microscopy (SEM). The presence of nanoparticles and other functional groups were observed from FT-IR results. Utilizing Debye-Scherer's equation, the outcome from the XRD investigation shows that the materials generated were on the nanoscale scale with a mean particle size of 32.49 nm. The absorbance maximum of produced nanoparticles was 264 nm and 376 nm, respectively, as determined by UV-vis spectroscopy. UV-vis spectroscopy was also used to investigate the optical characteristics of nanoparticles. The morphology of prepared ZnO NPs was evaluated by SEM shows flower images. Through the use of ZnO NPs on the surface of cotton textiles, the good performance of ZnO NPs as ultraviolet absorbers may be efficiently transferred to cotton textiles. The increase in UV absorption capacity of ZnO NP-treated cotton textiles, according to the ultraviolet-visible tests. The absorption capability of ZnO NPs on the surface of cotton textiles ensures that UV light is effectively shielded. The UV protection factor (UPF) and percentage of transmittance (percent T) values that have been computed reflect the protection offered by ZnO nanoparticles treated fabrics against ultraviolet light. This finding could be used to shield the body from the harmful effects of UV light.

Data Availability

The data used to support the findings of this study are included within the article.

Conflicts of Interest

The authors declare no conflict of interest.

References

[1] S. A. Noorian, N. Hemmatinejad, and J. A. Navarro, "Ligand modified cellulose fabrics as support of zinc oxide nanoparticles for UV protection and antimicrobial activities," *International Journal of Biological Macromolecules*, vol. 154, pp. 1215–1226, 2020.

[2] N. A. Ibrahim, A. A. Nada, B. M. Eid, M. Al-Moghazy, A. G. Hassabo, and N. Y. Abou-Zeid, "Synthesis, characterization and application of zinc oxide nanoparticles for textile materials against ultra violet radiation," *International Journal of Innovative Science and Research Technology*, vol. 9, article 035014, 2018.

[3] A. A. M. Attia, M. S. Antonious, M. A. H. Shouman, A. A. A. Nada, and K. M. Abas, "Processing and fundamental characterization of carbon fibers and cellulose nanocrystals derived from bagasse," *Carbon Letters*, vol. 29, no. 2, pp. 145–154, 2019.

[4] A. Rahdar, M. R. Hajinezhad, V. S. Sivasankarapillai, F. Askari, M. Noura, and G. Z. Kyzas, "Synthesis, characterization, and intraperitoneal biochemical studies of zinc oxide nanoparticles in Rattus norvegicus," *Applied Physics A*, vol. 126, no. 5, pp. 1–9, 2020.

[5] B. Abebe, B. Bulcha, and A. R. C. Reddy, "Effects of temperature and polyvinyl alcohol concentrations in the synthesis of zinc oxide nanoparticles," *Journal of Nanotechnology and Materials Science*, vol. 5, no. 1, pp. 44–50, 2018.

[6] M. E. el-Naggar, S. Shaarawy, and A. A. Hebeish, "Multifunctional properties of cotton fabrics coated with in situ synthesis of zinc oxide nanoparticles capped with date seed extract," *Carbohydrate Polymers*, vol. 181, pp. 307–316, 2018.

[7] A. Fouda, S. el-Din Hassan, S. S. Salem, and T. I. Shaheen, "_In-Vitro_ cytotoxicity, antibacterial, and UV protection properties of the biosynthesized Zinc oxide nanoparticles for medical textile applications," *Microbial Pathogenesis*, vol. 125, pp. 252–261, 2018.

[8] A. V. Abramova, V. O. Abramov, V. M. Bayazitov et al., "A sol-gel method for applying nanosized antibacterial particles to the surface of textile materials in an ultrasonic field," *Ultrasonics Sonochemistry*, vol. 60, p. 104788, 2020.

[9] W. Zhang, X. Chen, Y. Ma et al., "Positive aging effect of ZnO nanoparticles induced by surface stabilization," *The Journal of Physical Chemistry Letters*, vol. 11, no. 15, pp. 5863–5870, 2020.

[10] A. Awad, A. I. Abou-Kandil, I. Elsabbagh, M. Elfass, M. Gaafar, and E. Mwafy, "Polymer nanocomposites part 1," *Journal of Thermoplastic Composite Materials*, vol. 28, no. 9, pp. 1343–1358, 2015.

[11] A. Verbic, M. Gorjanc, and B. Simoncic, "Zinc oxide for functional textile coatings: recent advances," *Coatings*, vol. 9, no. 9, p. 550, 2019.

[12] B. S. Butola and A. Kumar, "Green chemistry based in-situ synthesis of silver nanoparticles for multifunctional finishing of chitosan polysaccharide modified cellulosic textile substrate," *International Journal of Biological Macromolecules*, vol. 152, pp. 1135–1145, 2020.

[13] H. Y. Phin, Y. T. Ong, and J. C. Sin, "Effect of carbon nanotubes loading on the photocatalytic activity of zinc oxide/carbon nanotubes photocatalyst synthesized via a modified sol-gel method," *Journal of Environmental Chemical Engineering*, vol. 8, no. 3, p. 103222, 2020.

[14] K. F. Hasan, H. Wang, S. Mahmud, and C. Genyang, "Coloration of aramid fabric via in-situ biosynthesis of silver

nanoparticles with enhanced antibacterial effect," *Inorganic Chemistry Communications*, vol. 119, p. 108115, 2020.

[15] U. Manzoor, M. Islam, L. Tabassam, and S. U. Rahman, "Quantum confinement effect in ZnO nanoparticles synthesized by co-precipitate method," *Physica E: Low-dimensional Systems and Nanostructures*, vol. 41, no. 9, pp. 1669–1672, 2009.

[16] A. H. Alrajhi, N. M. Ahmed, M. al Shafouri, M. A. Almessiere, and A. ahmed Mohammed al-Ghamdi, "Green synthesis of zinc oxide nanoparticles using salvia officials extract," *Materials Science in Semiconductor Processing*, vol. 125, p. 105641, 2021.

[17] A. K. Dikshit, P. Banerjee, N. Mukherjee, and P. Chakrabarti, "Theoretical optimization of double dielectric back reflector layer for thin c-Si based advanced solar cells with notable enhancement in MAPD," *Superlattices and Microstructures*, vol. 149, p. 106747, 2021.

[18] M. Fiedot-Toboła, M. Ciesielska, I. Maliszewska et al., "Deposition of zinc oxide on different polymer textiles and their antibacterial properties," *Materials*, vol. 11, no. 5, p. 707, 2018.

[19] J. A. Delezuk, D. E. Ramírez-Herrera, B. Esteban-Fernández de Ávila, and J. Wang, "Chitosan-based water-propelled micromotors with strong antibacterial activity," *Nanoscale*, vol. 9, no. 6, pp. 2195–2200, 2017.

[20] S. Nourbakhsh, "Self-cleaning and antibacterial properties of ZnO nanoparticles on cotton fabric treated with maleic acid," *Materials Science*, vol. 27, no. 1, pp. 90–95, 2021.

[21] A. Yadav, V. Prasad, A. A. Kathe et al., "Functional finishing in cotton fabrics using zinc oxide nanoparticles," *Bulletin of Materials Science*, vol. 29, no. 6, pp. 641–645, 2006.

[22] N. A. Ibrahim, A. A. Nada, B. M. Eid, M. Al-Moghazy, A. G. Hassabo, and N. Y. Abou-Zeid, "Nano-structured metal oxides: synthesis, characterization and application for multifunctional cotton fabric," *Advances in Natural Sciences: Nanoscience and Nanotechnology*, vol. 9, no. 3, p. 035014, 2018.

[23] R. Pandimurugan and S. Thambidurai, "UV protection and antibacterial properties of seaweed capped ZnO nanoparticles coated cotton fabrics," *International Journal of Biological Macromolecules*, vol. 105, Partt 1, pp. 788–795, 2017.

[24] J. A. Shirley, S. E. Florence, B. S. Sreeja, G. Padmalaya, and S. Radha, "Zinc oxide nanostructure-based textile pressure sensor for wearable applications," *Journal of Materials Science: Materials in Electronics*, vol. 31, no. 19, pp. 16519–16530, 2020.

[25] S. M. Costa, D. P. Ferreira, A. Ferreira, F. Vaz, and R. Fangueiro, "Multifunctional flax fibres based on the combined effect of silver and zinc oxide (Ag/ZnO) nanostructures," *Nanomaterials*, vol. 8, no. 12, p. 1069, 2018.

[26] M. T. Noman, N. Amor, M. Petru, A. Mahmood, and P. Kejzlar, "Photocatalytic behaviour of zinc oxide nanostructures on surface activation of polymeric Fibres," *Polymers*, vol. 13, no. 8, p. 1227, 2021.

[27] M. S. Choi, H. G. Na, G. S. Shim et al., "Simple and scalable synthesis of urchin-like ZnO nanoparticles via a microwave-assisted drying process," *Ceramics International*, vol. 47, no. 10, pp. 14621–14629, 2021.

[28] A. H. Patil, S. A. Jadhav, V. B. More et al., "A new method for single step sonosynthesis and incorporation of ZnO nanoparticles in cotton fabrics for imparting antimicrobial property," *Chemical Papers*, vol. 75, no. 3, pp. 1247–1257, 2021.

[29] D. Asmat-Campos, D. Delfín-Narciso, and L. Juarez-Cortijo, "Textiles functionalized with ZnO nanoparticles obtained by chemical and green synthesis protocols: evaluation of the type of textile and resistance to UV radiation," *Fibers*, vol. 9, no. 2, p. 10, 2021.

[30] M. Turemen, A. Demir, and Y. Gokce, "The synthesis and application of chitosan coated ZnO nanorods for multifunctional cotton fabrics," *Materials Chemistry and Physics*, vol. 268, p. 124736, 2021.

[31] S. Abel, L. Tesfaye Jule, F. Belay et al., "Application of Titanium Dioxide Nanoparticles Synthesized by Sol-Gel Methods in Wastewater Treatment," *Journal of Nanomaterials*, vol. 2021, p. 6, 2021.

[32] D. Kundu, C. Hazra, A. Chatterjee, A. Chaudhari, and S. Mishra, "Extracellular biosynthesis of zinc oxide nanoparticles using _Rhodococcus pyridinivorans_ NT2: Multifunctional textile finishing, biosafety evaluation and _in vitro_ drug delivery in colon carcinoma," *Journal of Photochemistry and Photobiology B: Biology*, vol. 140, pp. 194–204, 2014.

[33] A. Javed, J. Wiener, A. Tamuleviciene et al., "One step in-situ synthesis of zinc oxide nanoparticles for multifunctional cotton fabrics," *Materials*, vol. 14, no. 14, p. 3956, 2021.

[34] M. Afsharpour and S. Imani, "Preventive protection of paper works by using nanocomposite coating of zinc oxide," *Journal of Cultural Heritage*, vol. 25, pp. 142–148, 2017.

[35] M. Wasim, M. R. Khan, M. Mushtaq, A. Naeem, M. Han, and Q. Wei, "Surface modification of bacterial cellulose by copper and zinc oxide sputter coating for UV-resistance/antistatic/antibacterial characteristics," *Coatings*, vol. 10, no. 4, p. 364, 2020.

[36] S. Preethi, A. Anitha, and M. Arulmozhi, "A comparative analysis of the properties of zinc oxide (ZnO) nanoparticles synthesized by hydrothermal and sol–gel methods," *Indian Journal of Science and Technology*, vol. 9, no. 40, pp. 1–6, 2016.

[37] G. Baskar, J. Chandhuru, K. S. Fahad, and A. S. Praveen, "Mycological synthesis, characterization and antifungal activity of zinc oxide nanoparticles," *Asian Journal of Pharmacy and Technology*, vol. 3, no. 4, pp. 142–146, 2013.

[38] M. D. Jayappa, C. K. Ramaiah, M. A. P. Kumar et al., "Green synthesis of zinc oxide nanoparticles from the leaf, stem and in vitro grown callus of Mussaenda frondosa L.: characterization and their applications," *Applied Nanoscience*, vol. 10, no. 8, pp. 3057–3074, 2020.

[39] B. Siripireddy and B. K. Mandal, "Facile green synthesis of zinc oxide nanoparticles by _Eucalyptus globulus_ and their photocatalytic and antioxidant activity," *Advanced Powder Technology*, vol. 28, no. 3, pp. 785–797, 2017.

[40] G. Sangeetha, S. Rajeshwari, and R. Venckatesh, "Green synthesis of zinc oxide nanoparticles by _aloe barbadensis miller_ leaf extract: Structure and optical properties," *Materials Research Bulletin*, vol. 46, no. 12, pp. 2560–2566, 2011.

[41] M. M. AbdElhady, "Preparation and characterization of chitosan/zinc oxide nanoparticles for imparting antimicrobial and UV protection to cotton fabric," *International Journal of Carbohydrate Chemistry*, vol. 2012, Article ID 840591, 6 pages, 2012.

[42] S. M. Taghizadeh, N. Lal, A. Ebrahiminezhad et al., "Green and economic fabrication of zinc oxide (ZnO) nanorods as a broadband UV blocker and antimicrobial agent," *Nanomaterials*, vol. 10, no. 3, p. 530, 2020.

[43] S. Abel, J. L. Tesfaye, R. Shanmugam et al., "Green synthesis and characterizations of zinc oxide (ZnO) nanoparticles using

aqueous leaf extracts of coffee (Coffea arabica) and its application in environmental toxicity reduction," *Journal of Nanomaterials*, vol. 2021, Article ID 3413350, 6 pages, 2021.

[44] A. Degefa, B. Bekele, L. T. Jule et al., "Green Synthesis, Characterization of Zinc Oxide Nanoparticles, and Examination of Properties for Dye-Sensitive Solar Cells Using Various Vegetable Extracts," *Journal of Nanomaterials*, vol. 2021, Article ID 3941923, 9 pages, 2021.

[45] A. M. Awwad, M. W. Amer, N. M. Salem, and A. O. Abdeen, "Green synthesis of zinc oxide nanoparticles (ZnO-NPs) using Ailanthus altissima fruit extracts and antibacterial activity," *Chemistry International*, vol. 6, no. 3, pp. 151–159, 2020.

[46] T. I. Shaheen, M. E. El-Naggar, A. M. Abdelgawad, and A. Hebeish, "Durable antibacterial and UV protections of in situ synthesized zinc oxide nanoparticles onto cotton fabrics," *International Journal of Biological Macromolecules*, vol. 83, pp. 426–432, 2016.

[47] R. K. Sharma and R. Ghose, "Synthesis of zinc oxide nanoparticles by homogeneous precipitation method and its application in antifungal activity against _Candida albicans_," *Ceramics International*, vol. 41, no. 1, pp. 967–975, 2015.